SIMILARITY SOLUTIONS OF COMPRESSIBLE FLOW OVER A ROTATING CONE WITH SURFACE SUCTION

by

Paul D. TOWERS and Stephen J. GARRETT*

Department of Mathematics & Department of Engineering,
University of Leicester, Leicester, UK

Original scientific paper
DOI: 10.2298/TSCI130408032T

We present solutions of the laminar compressible boundary-layer flows over the family of rotating cones subject to surface mass flux. The work is a generalization of previous studies of the compressible rotating-disk flow and incompressible rotating-cone flow without surface mass flux. Transformations are used which lead to a system of generalized von Karman equations with boundary conditions parameterized by half-angle and a mass-flux parameter. Results are discussed in terms of wall temperature and local Mach number in the particular case of air, although the formulation is readily extended to other fluids. It is suggested that suction acts a stabilizing mechanism, whereas increased wall temperature and local Mach number have destabilizing influences.

Key words: *rotating cone, compressible boundary-layer flow, similarity solution, surface mass flux*

Introduction

There have been many experimental and theoretical studies seeking to identify and understand the various instability mechanisms found in rotating 3-D boundary-layer flows. From the early work of Gregory [1] and Gregory and Walker [2] through to the more recent seminal work of Lingwood [3, 4] and beyond, the incompressible flow over a rotating disk has been extensively studied in the literature. Similarly, experimental work by Kreith *et al.* [5] as well as Tien and Campbell [6] has led to the recent theoretical studies of Garrett [7, 10], Garrett and Peake [8], Garrett *et al.* [9, 11], and Hussain *et al.* [12] wich are made progress in understanding the stability characteristics of the incompressible boundary-layer flow over rotating cones. However, despite Turkyilmazoglu *et al.* [13], and Turkyilmazoglu and Oygun [14], Turkyilmazoglu [15, 16] making significant progress in the study of compressible boundary-layer flows over rotating disks, there has been little work investigating the compressible rotating-cone flow. The motivation for this particular study is to generalize this body of previous work to examine the effect of compressibility on the boundary-layer flow over a rotating cone with general half-angle, ψ. This is motivated in part by recent advances in high-speed spinning projectiles and aeroengines where a better understanding of laminar-turbulent transition would potentially lead to an improvement in engineering designs. In particular, delaying transition over spinning projectiles could help

* Corresponding author; e-mail: stephen.garrett@leicester.ac.uk

reduce drag as well as having a positive effect on control and targeting, and will increase fuel efficiency by reducing drag in aeroengines.

Surface suction is well known to act as a stabilizing mechanism in related boundarylayer flows. For example, Gregory and Walker [2] discuss how the introduction of suction extends the laminar-flow region over a swept wing by reducing the thickness of the boundary layer and the magnitude of crossflow velocity. Furthermore, the literature on incompressible rotating-disk and related flows [4, 17-20] shows that suction has a stabilizing effect that results in increased critical Reynolds numbers for the onset of instability modes, a narrowing in the range of unstable parameters and a reduction in the amplification rates.

We ultimately aim towards stability analyses of the class of compressible rotating-cone flows, with surface suction considered as a potential stabilizing mechanism. However, to conduct the stability analyses, one must first compute the steady velocity profiles governing the laminar flow within the boundary layer. Obtaining the steady slows in the compressible case is significantly more complicated than in the incompressible case and warrants explicit consideration. This is the subject of this paper.

Derivation of the laminar flow equations

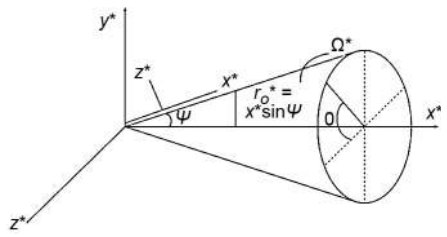

Figure 1. Geometrical set-up for the rotating cone

Consider a cone placed in an otherwise still compressible fluid, which rotates about its axis of symmetry with angular velocity, Ω^* (where superscript * denotes dimensional quantities). The angle between the cone's surface and its axis of symmetry is defined as the half-angle, ψ. The geometry is shown in fig. 1 and is formulated using Cartesian co-ordinates (X^*, Y^*, Z^*) with the origin placed at the tip of the cone. This is then transformed to the orthogonal curvilinear co-ordinates (x^*, θ, z^*) which represent the streamwise, azimuthal and a surface-normal co-ordinates, respectively. The co-ordinate transformation of the Cartesian system is given by:

$$X^* = x^* \cos\psi - z^* \sin\psi \tag{1}$$

$$Y^* = (x^* \sin\psi + z^* \cos\psi) \sin\theta \tag{3}$$

$$Z^* = (x^* \sin\psi + z^* \cos\psi) \cos\theta \tag{2}$$

The scale factors of the orthogonal curvilinear co-ordinates (x^*, θ, z^*) are given by $h_x = h_z = 1$ and $h_\theta = x^*\sin\psi + z^*\cos\psi = h^*$, where $r_0^* = x^*\sin\psi$ defines the local surface radius of the cone. This formulation is consistent with the literature on the equivalent but incompressible case [7-12, 21]. The method for the compressible case that follows here is a generalization of work by Turkyilmazoglu and Uygun [14] in the particular case of a rotating disk, where $\psi = 90°$. We note the recent work of Garrett *et al.* [9, 11], and Hussain *et al.* [12, 22], that suggests that a different formulation is required for slender cones with $\psi < 40°$. This has not yet been fully understood and we have therefore restricted the discussion to half-angles to broad cones, $\psi \geq 40°$.

The governing equations, consisting of the continuity equation, the Navier-Stokes equations, a state equation, and the energy equation are applied in a reference frame rotating with angular velocity Ω^* about the X*-axis. These are given by:

$$\frac{\partial \rho^*}{\partial t} + \nabla^* (\rho^* \vec{u}^*) = 0 \tag{4}$$

$$\frac{\mathrm{D}\vec{u}^*}{\mathrm{D}t} + 2\vec{\Omega}^*\vec{u}^* + (\vec{\Omega}\,\vec{\Omega}^*)\vec{r}^* = \frac{1}{\rho^*}\left[-\nabla^* p^* + \nabla^*(\lambda^* \nabla^* \vec{u}^*) + \nabla^*\left(\mu^* \sum_{j=1}^{3} \mathbf{e}_{i,j} \right) \right] \tag{5}$$

$$\gamma \mathrm{M}_\infty^2 p^* = \rho^* T^* \tag{6}$$

$$\rho^* \frac{\mathrm{D}h^*}{\mathrm{D}t^*} = \frac{\mathrm{D}p^*}{\mathrm{D}t^*} + \nabla^*(k^* \nabla^* T^*) + \mu^*(2\mathbf{e}_{11}^2 + 2\mathbf{e}_{22}^2 + 2\mathbf{e}_{33}^2 + 2\mathbf{e}_{12}^2 + 2\mathbf{e}_{13}^2 + 2\mathbf{e}_{23}^2) + \\ + \lambda^*(\nabla^* \vec{u}^*)^2 \tag{7}$$

where the Coriolis forcing term $2\vec{\Omega}^*\vec{u}^*$ appears due to the rotating frame of reference. Note that this is in contrast to Garrett's [7] formulation that uses a stationary frame. The vector $\vec{u}^* = (u^*, v^*, w^*)$ denotes the velocity flow field and $\vec{r}^* = (x^*, 0, z^*)$ gives the position vector. The parameters given in eqs. (4)-(7) are defined: ρ^* is the density, p^* – the pressure; λ^* – the second coefficient of viscosity related to the bulk viscosity, μ^* – the dynamic viscosity, M_∞ – the free-stream Mach number, T^* – the temperature, and h – the enthalpy. The heat capacity ratio γ is the ratio of the heat capacity at constant pressure c_p to the heat capacity at constant volume c_v. The parameter k^* is that associated with the Prandtl number, Pr, where $k^*\mathrm{Pr} = c_p\mu^*$. The components of the strain tensor $\mathbf{e}_{ij}$ are given by:

$$\mathbf{e}_{11} = \frac{\partial u^*}{\partial x^*}$$

$$\mathbf{e}_{12} = \mathbf{e}_{21} = \frac{1}{2}\left(\frac{\partial v^*}{\partial x^*} + \frac{1}{h^*}\frac{\partial v^*}{\partial \theta} - \frac{v^* \sin\psi}{h^*} \right)$$

$$\mathbf{e}_{13} = \mathbf{e}_{31} = \frac{1}{2}\left(\frac{\partial w^*}{\partial x^*} + \frac{\partial u^*}{\partial z^*} \right)$$

$$\mathbf{e}_{22} = \frac{1}{h^*}\frac{\partial v^*}{\partial \theta} + \frac{w^* \cos\psi}{h^*} + \frac{u^* \sin\psi}{h^*}$$

$$\mathbf{e}_{23} = \mathbf{e}_{32} = \frac{1}{2}\left(\frac{\partial v^*}{\partial z^*} + \frac{1}{h^*}\frac{\partial w^*}{\partial \theta} - \frac{v^* \cos\psi}{h^*} \right)$$

$$\mathbf{e}_{33} = \frac{\partial w^*}{\partial z^*}$$

The resulting dimensional governing equations are stated by Towers [23]. Equations (4)-(7) are subject to appropriate boundary conditions on the cone surface and in the far field:

$$u^* = 0, \quad v^* = 0, \quad w^* = \bar{a}^*, \quad T^* = T_w^* \quad \text{on} \quad z^* = 0$$

$$u^* \to 0, \quad v^* \to -x^*\Omega^* \sin\psi, \quad T^* \to T_\infty \quad \text{as} \quad z^* \to \infty$$

where $\bar{a}^*$ is the suction parameter, T_w^* – the temperature of the cone surface, and subscript ∞ denotes the free stream value of the variable.

The characteristic length along the cone surface, l^*, is used to scale any length quantities and the surface normal co-ordinate is further scaled using the modified boundary-layer thickness. This leads to non-dimensional spatial variables:

$$x^* = l^* x, \qquad z^* = l^* z, \qquad z = \sqrt{\mathrm{Re}}\eta$$

where Re is the Reynolds number given by:

$$\mathrm{Re} = \frac{\rho^* l^{*2} \Omega^* \sin\psi}{\mu^*} \tag{8}$$

The velocity quantities are scaled:

$$(u^*, v^*, w^*) = l^* \Omega^* \sin\psi (u, v, \sqrt{\mathrm{Re}} w)$$

with the pressure given by $p^* = p^* I^* \Omega^* \sin\psi p$. All other variables are scaled using their free-stream values. Again, this method is consistent with Turkyilmazoglu and Uygun [14] in the particular case of $\psi = 90°$ and $a^* = 0$.

To obtain the governing steady axisymmetric mean flow equations we neglect any dependence on time and the azimuthal co-ordinate, θ, and non-dimensionalise eqs. (4)-(7). We then expand in terms of R and dismiss terms of $O(\mathrm{Re}^{-1/2})$ due to the assumption of large Reynolds number. Physically this limits the analysis to high rotation rates and/or large characteristic length scales relative to the boundary-layer thickness. This leads to the reduced system of non-dimensional equations:

$$u\frac{\partial p}{\partial x} + w\frac{\partial \rho}{\partial \eta} + \rho\left(\frac{\partial u}{\partial x} + \frac{\partial w}{\partial \eta}\right) + \frac{\partial u}{x} = 0 \tag{9}$$

$$\rho\left(u\frac{\partial u}{\partial x} + w\frac{\partial u}{\partial \eta} - \frac{v^2}{x} - 2v - x\right) = -\frac{\partial p}{\partial x} + \frac{\partial}{\partial \eta}\left(\mu\frac{\partial u}{\partial \eta}\right) \tag{10}$$

$$\rho\left(u\frac{\partial v}{\partial x} + w\frac{\partial v}{\partial \eta} + \frac{uv}{x} + 2u\right) = \frac{\partial}{\partial \eta}\left(\mu\frac{\partial v}{\partial \eta}\right) \tag{11}$$

$$\mathrm{ctg}\psi\left(\frac{v^2}{x} + 2v + x\right) = \frac{\partial p}{\partial \eta} \tag{12}$$

$$\gamma \mathrm{M}_\infty^2 p = \rho T \tag{13}$$

$$\rho\left(u\frac{\partial T}{\partial x} + w\frac{\partial T}{\partial \eta}\right) = \mathrm{M}_\infty^2(\gamma - 1)\left\{u\frac{\partial p}{\partial x} + w\frac{\partial p}{\partial \eta} + \mu\left[\left(\frac{\partial u}{\partial \eta}\right)^2 + \left(\frac{\partial v}{\partial \eta}\right)^2\right]\right\} + \frac{\partial}{\partial \eta}k\frac{\partial T}{\partial \eta} \tag{14}$$

subject to the boundary conditions:

$$u = 0, \quad v = 0, \quad w = \frac{\overline{a}}{\sin\psi} \quad \text{on} \quad \eta = 0$$
$$u \to 0, \quad v \to -x\sin\psi \quad \text{as} \quad \eta \to 0 \tag{15}$$
$$\rho, T, \mu \to 1, \quad p \to \frac{1}{\gamma \mathrm{M}_\infty^2} \quad \text{as} \quad \eta \to \infty$$

Note that the velocity scalings are such that the surface mass flux condition now depends on ψ. We note that the normal component of the flow, w, is of order $O(\mathrm{Re}^{-1/2})$, our analysis therefore proceeds with a focus on the leading order effects arising from the streamwise and azimuthal components only. As previously explained, this limits the study to high rotation rates. Work into the stability of the incompressible boundary-layer flows over rotating cones [7-9] has shown that the normal component has only a marginal qualitative effect on the stability properties. This approximation in our analysis, although not entirely physical as the normal component is of course required for growth of the boundary layer, is therefore reasonable.

Solution of the governing equations

To proceed in reducing the governing equations to a von Karman type similarity solution we make further assumptions. We let the fluid satisfy Chapman's viscosity law, that is $\mu = CT$ for some constant C. As a constant, C can be mathematically absorbed into the definition of μ without a loss of generality in the analysis that follows; this is equivalent to choosing $C = 1$. We remove the density terms from the equations using a Dorotonitsyn-Howarth transformation, shown by Stewartson [24] and given by:

$$y = \int_0^\eta \rho \mathrm{d}\eta \tag{16}$$

The velocity and pressure quantities are then further scaled using:

$$(u, v, w, p) = [xU(y), xV(y), W(y), (\gamma \mathrm{M}_\infty^2)^{-1}]$$

We introduce a stream function satisfying eq. (4) and given by:

$$U = \frac{\mathrm{d}\Psi}{\mathrm{d}y} = \Psi'(y), \qquad W = T\left(2\Psi + x\Psi'\frac{\partial y}{\partial x}\right)$$

Applying this to eqs. (9)-(14) leads to the generalized set of von Karman equations for the compressible boundary-layer flow over a rotating cone:

$$\Psi''' = \Psi'^2 - 2\Psi\Psi'' - (V+1)^2 \tag{17}$$

$$V'' = 2(V+1)\Psi' - 2\Psi V \tag{18}$$

$$\frac{\partial^2 T}{\partial y^2} + 2\,\mathrm{Pr}\,\Psi\frac{\partial T}{\partial y} - x\,\mathrm{Pr}\,\Psi'\frac{\partial T}{\partial x} + (\gamma-1)\,\mathrm{Pr}\,x^2\mathrm{M}_\infty^2(\Psi''^2 + V^2) = 0 \tag{19}$$

subject to the boundary conditions:

$$\Psi(0) - \frac{a}{\sin\psi} = \Psi'(0) = \Psi(\infty) = 0, \qquad V(0) = V(\infty) + 1 = T(\infty) - 1 = 0 \tag{20}$$

where $a = -\bar{a}/2T_w$ is the modified mass-flux parameter and is considered for $-1 \le a \le 1$. Note that $a > 0$ represents suction through the cone surface and $a < 0$ injection. The prime indicates a spatial derivative with respect to y.

It is seen that compressibility leads to a system defined by the standard von Karman eqs. (17) and (18), and the energy equation (19) where the effects of compressibility are confined. To proceed further we follow [25] and rewrite this partial differential equation as two ODE *via* the temperature relation:

$$T = 1 - \frac{\gamma - 1}{2} \mathrm{M}_x^2 f(y) + (T_w - 1) q(y) \tag{21}$$

where f is a viscous dissipation quantity, q – the heat conduction term and M_x – the local Mach number defined by $\mathrm{M}_x = x \sin \psi \mathrm{M}_\infty$. Equation (19) is then expressed:

$$f'' + 2\,\mathrm{Pr}\,\Psi f' - 2\,\mathrm{Pr}\,\Psi' f = 2\,\mathrm{Pr}(\Psi''^2 + V'^2) \tag{22}$$

$$q'' + 2\,\mathrm{Pr}\,\Psi q' = 0 \tag{23}$$

The free flow uniform temperature from condition (20), along with the heat transfer at the wall, leads to the boundary conditions:

$$f(0) = f(\infty) = q(0) - 1 = q(\infty) = 0 \tag{24}$$

We note that the governing eqs. (17)-(24) are identical to those presented by Turkyilmazoglu and Oygun [14] for the rotating-disk flow, dependence on cone half-angle has been removed by a careful choice of scalings. Furthermore, the effects of surface mass flux appear in the surface boundary conditions only.

Results and discussion

Zero mass flux

We begin by considering the simple case of zero surface mass flux and set $a = 0$. An implicit fourth-order Runge-Kutta integration method is used to numerically solve eqs. (17) and (18) subject to:

$$\Psi(0) = \Psi'(0) = \Psi(\infty) = 0, \qquad V(0) = V(\infty) + 1 = T(\infty) - 1 = 0$$

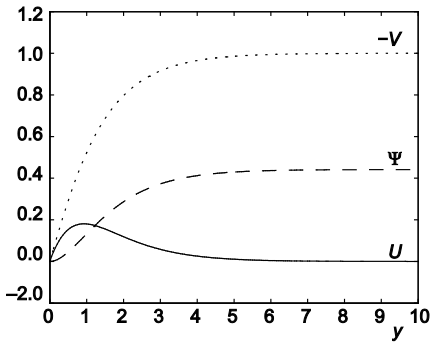

Figure 2. Distribution of Ψ, *U*, and –*V* across the boundary layer

Figure 2 shows the solution for the stream function and the streamwise and negative azimuthal components of the steady laminar flow velocity within the boundary layer. Of course, these are identical to those resulting from studies of the incompressible flow over the rotating disk as the effects of both compressibility and half-angle have been removed by the Dorotonitsyn-Howarth transformation (16) and appropriate scalings. We will recover the physical effects of compressibility and half-angle in the chapter *Physical interpretation*.

Using the numerical solutions for $\Psi(y)$, $\Psi'(y)$, and $V(y)$ shown in fig. 2, we proceed to solve ODE (22) and (23) subject to the boundary conditions

(20) and (24) to obtain the temperature profiles. For illustration, we assume the compressible fluid to be air and set Pr = 0.7 and γ = 1.4. Figure 3 shows the temperature distributions for two cases of constant local Mach number at various wall temperature, agreement with Turkyilmazoglu *et al.* [13] is found for M_x = 1.

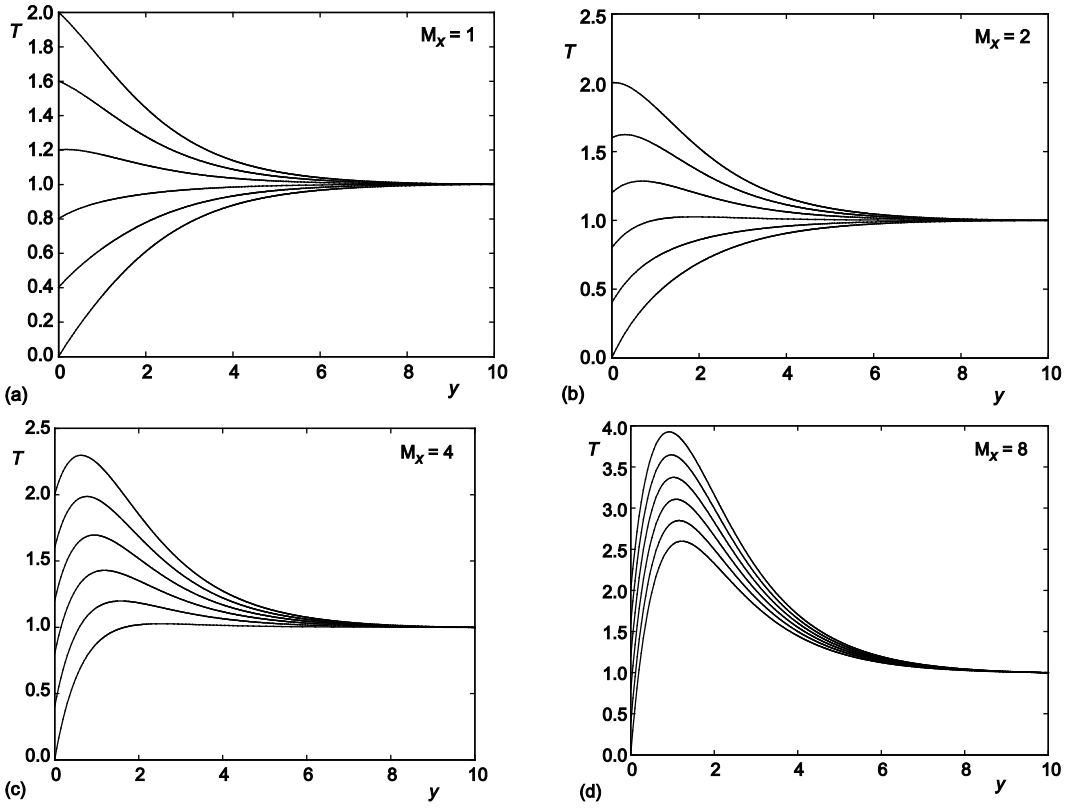

Figure 3. Temperature distribution across the boundary layer for M_x =1, 2, 4, and 8 and various wall temperatures; the wall temperature increases vertically from 0 to 2 in increments of 0.4

The effect of the quadratic local Mach number in eq. (21) is clear. For M_x = 1 the temperature distributions all tend to unity (the scaled free-stream temperature) with no turning point. For larger M_x and sufficient T_w we find that the temperature profiles grow to a maximum before tending to the scaled free-stream value. Figure 4 shows the temperature distributions for several cases of constant wall temperature at various local Mach number. Again, the local Mach number is seen to be the dominant parameter and a substantial difference in the temperature at locations near to the wall can be seen at different M_x for each fixed T_w.

Non-zero mass flux

Figure 5 shows the steady-flow profiles resulting from a uniform suction along the surface of the cone for various values of the half-angle ψ and suction parameter a, the wall temperature is fixed at T_w = 0.5. The ψ-dependence arises through the normal velocity boundary condition (20) and is necessary to ensure that a particular value of the suction parameter a represents the same physical surface mass flux across all ψ. Whilst the half angle is shown to

have an effect on the stream function, the velocity components U and V are relatively insensitive to this change. Suction is seen to narrow the boundary layer in this scaled normal co-ordinate, as would be expected, and also reduces the magnitude of crossflow velocity. Both of these are expected to have a stabilizing effect on the physical flows.

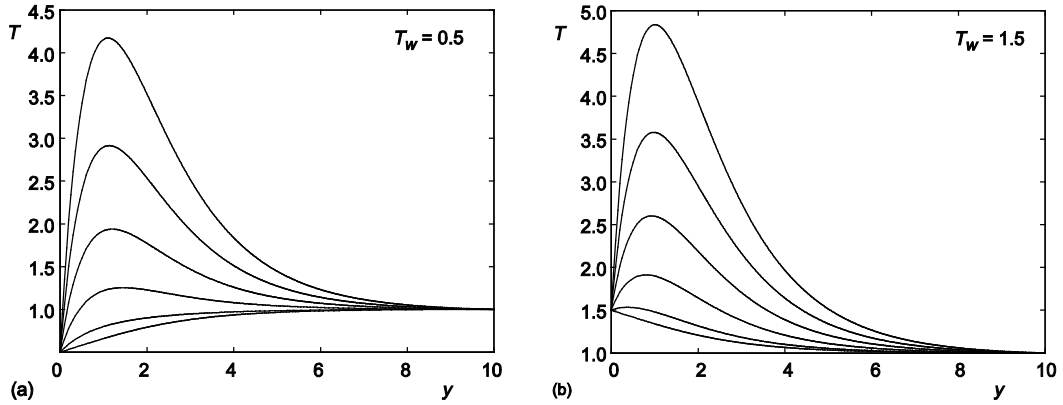

Figure 4. Temperature distribution across the boundary layer for T_w = 0.5 and 1.5 and various Mach numbers; the Mach number increases vertically from 0 to 10 in increments of 2

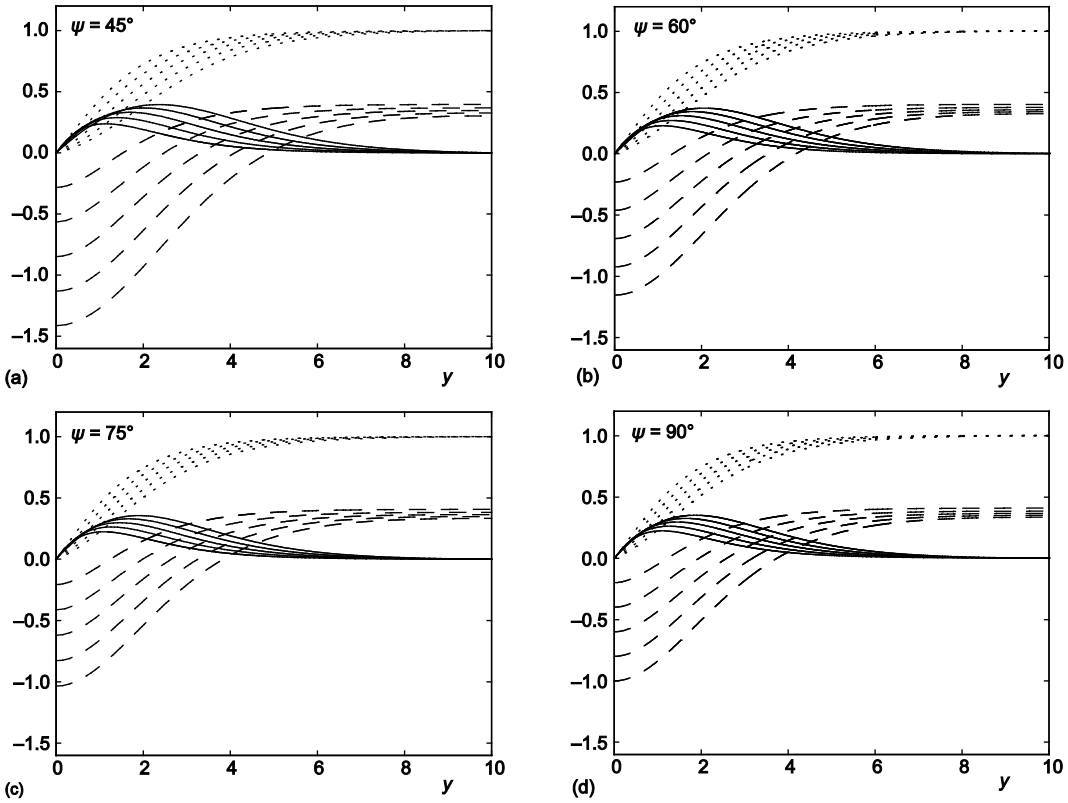

Figure 5. Varying suction parameter, increasing vertically from $\bar{a}$ = –1 to $\bar{a}$ = –0.2 in increments of 0.2, for several cone half angles, where Ψ (– –), U (—), and V (····)

Physical interpretation

To recover the physical spatial quantity, z, we invert transformation (16) used to eliminate the density terms and substitute eq. (21). By defining $\mathrm{Re} = \sin\psi \mathrm{Re}_{90}$, where Re_{90} is the Reynolds number in the disk case and is used as a normalising factor, we obtain:

$$z = \frac{1}{\sqrt{(\sin\psi)}}\left[y - \frac{\gamma - 1}{2} \mathrm{M}_x^2 \int_0^y f \,\mathrm{d}y + (T_w - 1) \int_0^y q \,\mathrm{d}y \right]$$

This reintroduces several physical parameters that were previously scaled out, namely wall temperature, cone half-angle and local Mach number, and facilitates a study of the physical effects of compressibility.

Figure 6 shows the effect of local Mach number and surface suction on the laminar flow profiles for $T_w = 1$. Similarly, fig. 7 shows the change brought by a change in the wall temperature and surface suction for $\mathrm{M}_x = 1$. Compressibility is seen to have a stretching effect on the flow profiles due to the quadratic local Mach number term, with the wall temperature controlling the magnitude of the heat conduction integral term. An increase in either local Mach number or wall temperature are seen to broaden the boundary layer, and suction narrows it.

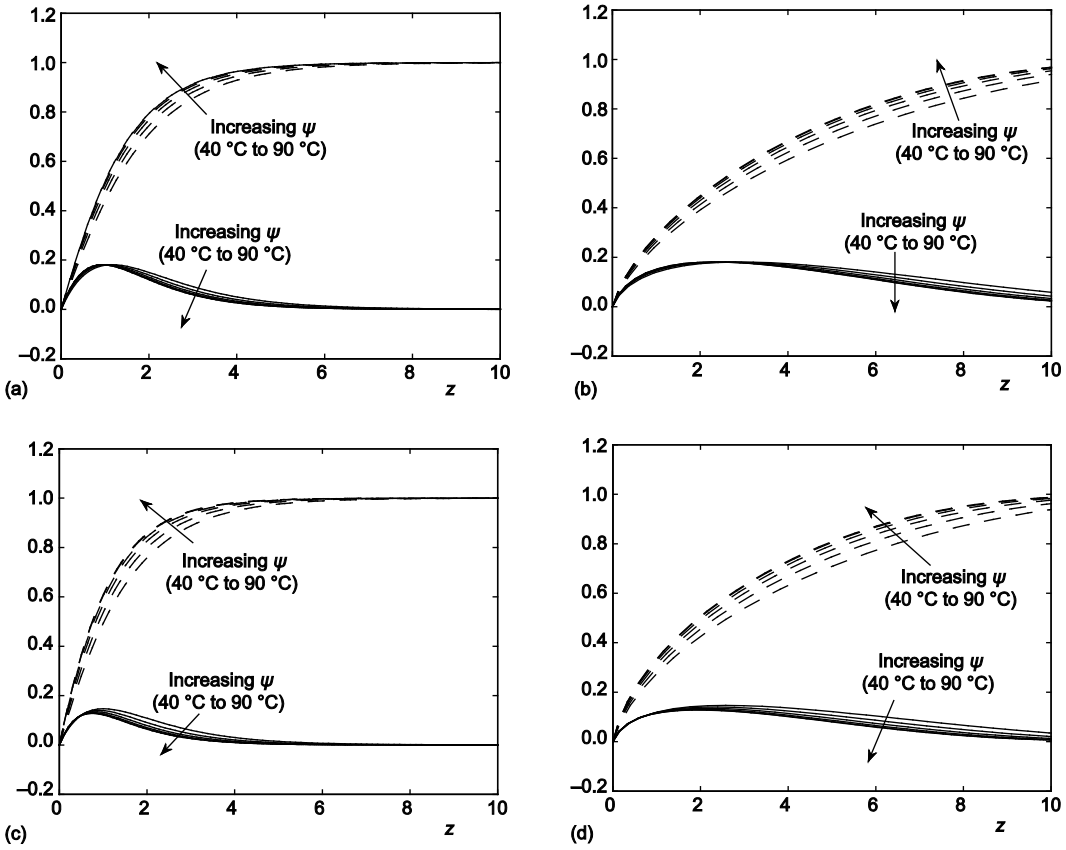

Figure 6. Physical laminar flow profiles U (—), V (⋯) for $\psi = 40°$-$90°$, $T_w = 1$ with: (a) $\bar{a} = 0$, $\mathrm{M}_x = 0.5$, (b) $\bar{a} = 0$, $\mathrm{M}_x = 8$, (c) $\bar{a} = -0.5$, $\mathrm{M}_x = 0.5$, and (d) $\bar{a} = -0.5$, $\mathrm{M}_x = 8$

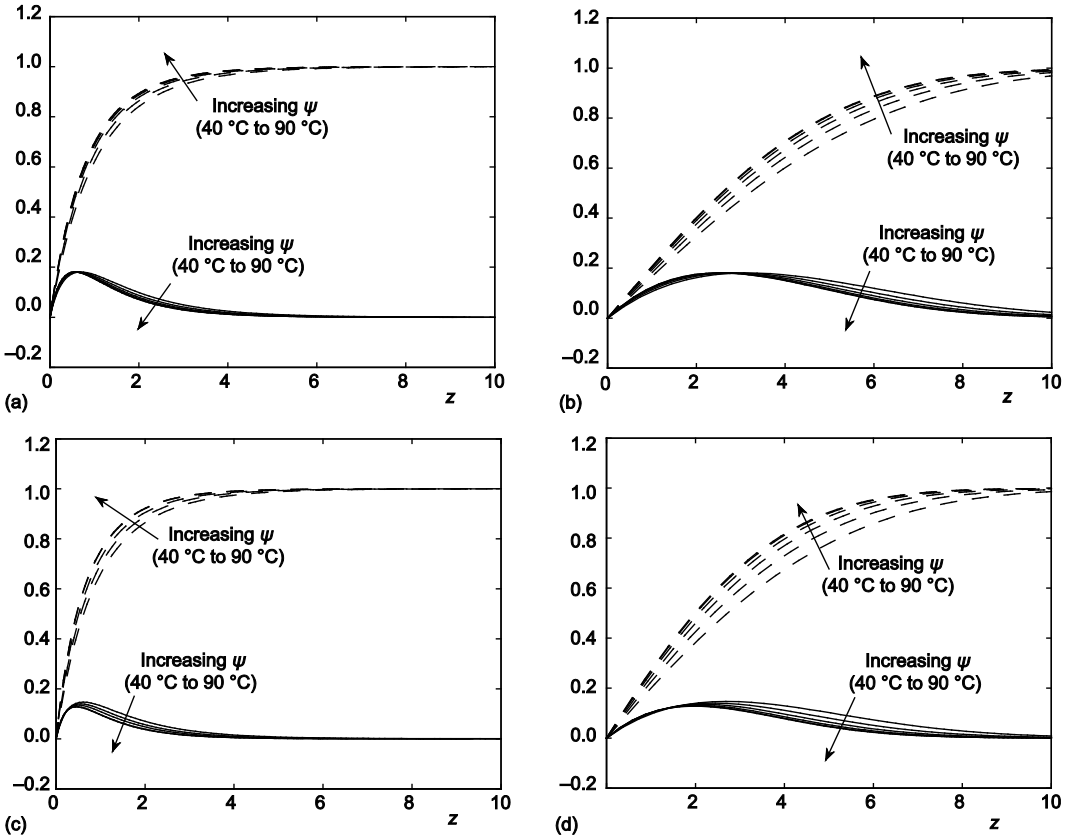

Figure 7. Physical laminar flow profiles U (—), V (····) for $\psi = 40°$-$90°$, $M_x = 1$ with: (a) $\bar{a} = 0$, $T_w = 0.5$, (b) $\bar{a} = 0$, $T_w = 3$, (c) $\bar{a} = -0.5$, $T_w = 0.5$, and (d) $\bar{a} = -0.5$, $T_w = 3$

For illustration, all results have been presented for air, thereby fixing Pr = 0.7 and $\gamma = 1.4$. Most gases have values of Pr ≈ 0.16-0.8 and $\gamma \approx$ 1-1.7, and changes in these parameters would cause little change in our results.

Conclusions

We have established the generalized von Karman equations for the compressible boundary-layer flow over a rotating cone subject to surface mass flux under the assumption of large Reynolds number. The resulting ODE have been solved numerically to generate scaled streamwise and azimuthal components of the steady velocity flow field via a stream function. The choice of scalings has enabled the cone half-angle to be factored out and we obtain expressions identical to those for the compressible flow over a rotating disk.

The resulting flow profiles have been recast in terms of the physical spatial normal co-ordinate to consider the physical effects of the local Mach number and wall temperature. An increase in either parameter is shown to broaden the boundary layer and both are therefore expected to be *destabilizing* influences. Increased suction is shown to narrow the boundary layer and reduce the magnitude of crossflow velocity for all combinations of flow parameters. Surface suction is therefore expected to be a *stabilizing* influence, consistent with previous studies of related rotating flows in the literature.

Acknowledgments

This on-going work is supported by the Engineering and Physical Sciences Research Council (grant EP/G061637/1).

Nomenclature

Many variables appear in both their dimensional and non-dimensional forms. A dimensional quantity is indicated with an asterisk.

$\bar{a}^*$ – suction parameter, [ms^{-1}]
a – transformed suction parameter, [–]
$\mathbf{e}_{ij}$ – strain tensor components, [–]
f – dissipative quantity, [–]
h – enthalpy, [J]
h^*_x, h^*_g, h^*_z – scale factors, [m]
k – thermal conductivity, [Wm^{-1}K^{-1}]
l^* – characteristic length scale, [m]
M_∞ – free-stream Mach number, [–]
M_x – local Mach number, [–]
Pr – Prandtl number, [–]
p^* – pressure, [Pa]
q – heat conduction term, [–]
$\bar{r}^*$ – position vector [= (x^*, θ, z^*)], [m]
r_0^* – local surface radius, [m]
Re – Reynolds number
[= $(\rho^* l^{*2} \Omega^* \sin\psi)/\mu^*$], [–]
T^* – temperature, [K]
T_w^*, T_∞^* – temperature boundary conditions, [K]
$\bar{u}^*$ – velocity vector [= (u^*, v^*, w^*)], [ms^{-1}]
U, V, W – transformed velocity vector, [–]
y – transformed normal co-ordinate, [–]

Greek symbols

γ – ratio of heat capacities [= c_p/c_v], [–]
η – non-dimensional normal distance, [–]
λ^* – second coefficient of viscosity, [Pa·s]
μ^* – dynamic viscosity, [Pa·s]
ρ^* – fluid density, [kgm^{-3}]
Ψ – stream function, [–]
ψ – cone half-angle, [°]
Ω^* – angular velocity, [s^{-1}]

References

[1] Gregory, N., *et al.*, On the Stability of Three-Dimensional Boundary Layers with Application to the Flow Due to a Rotating Disk, *Phil. Trans. R. Soc. Lond.* A *248*, (1955), 943, pp. 155-199
[2] Gregory, N., Walker, W. S., Experiments on the Effect of Suction on the Flow Due to a Rotating Disk, *Journal of Fluid Mechanics, 9* (1960), 2, pp. 225-234
[3] Lingwood, R. J., Absolute Instability of the Boundary Layer on a Rotating Disk, *J. Fluid Mech., 299*, (1995), Sep., pp. 17-33
[4] Lingwood, R. J., On the Effects of Suction and Injection on the Absolute Instability of a Rotating Disk Boundary Layer, *Phys. Fluids, 9* (1997), 5, pp. 1317-1328
[5] Kreith, F., *et al.*, An Experimental Investigation of the Flow Engendered by a Rotating Cone, *Appl. Sci. Res., A11*, (1962), 4, pp. 430-440
[6] Tien, C. L., Campbell, D. T., Heat and Mass Transfer from Rotating Cones, *J. Fluid Mech., 17* (1963), 1, pp. 105-112
[7] Garrett, S. J., The Stability and Transition of the Boundary Layer on Rotating Bodies, Ph. D. thesis, Cambridge University, Cambridge, UK, 2002
[8] Garrett, S. J., Peake, N., The Absolute Instability of the Boundary Layer on a Rotating Cone, *European J. Mech. B., 26* (2007), 3, pp. 344-353
[9] Garrett, S. J., *et al.*, The Crossflow Instability of the Boundary Layer on a Rotating Cone, *J. Fluid Mech., 622* (2009), Mar., pp. 209-232
[10] Garrett, S. J., Linear Growth Rates of Types I & II Convective Modes within the Rotating-Cone Boundary Layer, *Fluid Dyn. Res., 42* (2010), 2, pp. 025504-025515
[11] Garrett, S. J., *et al.*, Boundary-Layer Transition on Broad Cones Rotating in an Imposed Axial Flow, *AIAA Journal*, *48* (2010), 6, pp. 1184-1194
[12] Hussain, Z., *et al.*, The Centrifugal Instability of a Slender Rotating Cone, *Journal of Algorithms & Computational Technology*, *6* (2012), 1, pp. 113-128
[13] Turkyilmazoglu, M., *et al.*, Absolute and Convective Instabilities in the Compressible Boundary Layer on a Rotating Disk, *Theor. Comput. Fluid Dyn., 14* (2000), 1, pp. 21-37

[14] Turkyilmazoglu, M., Uygun, N., Basic Compressible Flow over a Rotating Disk, *Hace. J. Math. Stat., 33* (2004), 1, pp. 1-10
[15] Turkyilmazoglu, M., Lower Branch Modes of the Compressible Boundary Layer Flow Due to a Rotating Disk, *Stud. Appl. Math., 114* (2005), 1, pp. 17-43
[16] Turkyilmazoglu, M., Influence of Finite Amplitude Disturbances on the Nonstationary Modes of a Compressible Boundary Layer Flow, *Stud. Appl. Math., 118* (2007), 3, pp. 199-220
[17] Lingwood, R. J., Garrett, S. J., The Effects of Surface Mass Flux on the Instability of the BEK System of Rotating Boundary-Layer Flows, *European J. Mech. B.*, *30* (2011), 3, pp. 299-310
[18] Ockendoh, H., An Asymptotic Solution for Steady Flow above an Infinite Rotating Disc with Suction, *Q. J. Mech. appl. Math.*, *25* (1971), 3, pp. 291-301
[19] Bassom, A. P., Seddougui, S. O., The Effects of Suction on the Nonlinear Stability of ohe Three-Dimensional Boundary Layer above a Rotating Disk, *Proc. R. Soc. Lond. A*, *436* (1992), 1897, pp. 405-415
[20] Dhanak, M. R., Effects of Uniform Suction on the Stability of flow on a Rotating Disk, *Proc. R. Soc. Lond. A*, *439* (1992), 1906, pp. 431-440
[21] Hussain, Z., Stability and Transition of Three Dimensional Rotating Boundary Layers, Ph. D. thesis, University of Birmingham, West Midlands, UK, 2009
[22] Hussain, Z., *et al.*, Distinct Transition Mechanisms over Slender and Broad Rotating Cones, *Proceedings,* 40th AIAA Fluid Dynamics Conference, Chicago, Ill., USA, AIAA-2010-4285
[23] Towers, P. D., The Stability and Transition of the Compressible Boundary-Layer Flow over Broad Rotating Cones, Ph. D. thesis, University of Leicester, Leicester, UK, 2013
[24] Stewartson, K., *The Theory of Laminar Boundary Layers in Compressible Fluids,* Oxford University Press, Oxford, UK, 1964
[25] Riley, N., The Heat Transfer from a Rotating Disk, *Q. J. Mech. Appl. Math., 17* (1964), 3, pp. 331-349

Paper submitted: April 8, 2013
Paper revised: November 11, 2013
Paper accepted: March 3, 2014